

See discussions, stats, and author profiles for this publication at: <https://www.researchgate.net/publication/259934552>

Spin-Crossover Anticooperativity Induced by Weak Intermolecular Interactions

ARTICLE *in* JOURNAL OF PHYSICAL CHEMISTRY LETTERS · JANUARY 2014

Impact Factor: 7.46 · DOI: 10.1021/jz402678q

CITATIONS

9

READS

51

6 AUTHORS, INCLUDING:



[Ivan V. Ananyev](#)

Russian Academy of Sciences

40 PUBLICATIONS 106 CITATIONS

[SEE PROFILE](#)



[Konstantin A Lyssenko](#)

Russian Academy of Sciences

761 PUBLICATIONS 6,128 CITATIONS

[SEE PROFILE](#)



[Yan Z Voloshin](#)

Russian Academy of Sciences

92 PUBLICATIONS 1,082 CITATIONS

[SEE PROFILE](#)

Spin-Crossover Anticooperativity Induced by Weak Intermolecular Interactions

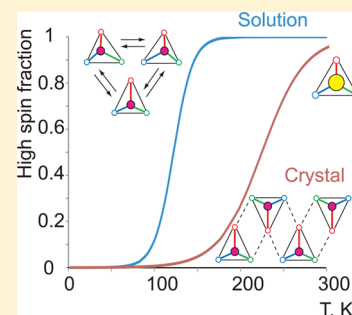
Valentin V. Novikov,[†] Ivan V. Ananyev,[†] Alexander A. Pavlov,[†] Matvey V. Fedin,[‡] Konstantin A. Lyssenko,[†] and Yan Z. Voloshin^{*,†}

[†]Nesmeyanov Institute of Organoelement Compounds RAS Vavilova, 28, Moscow 119991, Russia

[‡]International Tomography Center, SB RAS, Institutskaya 3A, Novosibirsk 630090, Russia

Supporting Information

ABSTRACT: As a rule, rational design of cooperative spin-crossover (SCO) molecular switches is largely based on consideration of sizes and structures of individual building blocks, whereas a meticulous analysis of crystal packing, including the weakest intermolecular interactions, is often assumed to play a secondary role or is even fully neglected. By investigating cobalt(II) clathrochelates, which do not change the molecular volume upon SCO, we showed that even weak (1.2 kcal/mol) $\pi \cdots \text{Cl}$ intermolecular interactions can cause a pronounced anticooperativity of SCO, being more gradual in the solid state than in solution. Our results clearly demonstrate that the “chemical pressure” concept is not as general as it is thought to be, and the successful design of molecular switches requires in-depth analysis of intermolecular interactions, however weak they seem.



SECTION: Molecular Structure, Quantum Chemistry, and General Theory

Spin-crossover (SCO) complexes^{1,2} are very popular in the area of molecular electronics^{3–5} owing to the long-recognized possibility of using the energy difference between low-spin (LS) and high-spin (HS) states of a transition-metal ion to create a molecular switch.^{6,7} As in most cases, temperature-induced SCO has an intrinsically statistical nature, it is hard to obtain a purely two-state molecular switch.⁸ In solids, however, the cooperative effects often lead to the hysteresis in SCO curves, allowing discrimination between purely LS and HS states.⁹ It is generally accepted now that the cooperativity in SCO is a result of elastic interactions,¹⁰ meaning that the increase in the molecular volume during SCO creates a “chemical pressure” that then propagates through the crystal via phonon interactions.² Although in most cases this model allows for a quantitative description of the SCO curves,¹¹ its application in rational design of molecular switches is not immediately recognized. The molecular structure-based approach¹² suggests that the cooperative effects originate from specific changes in the molecular shapes and also accounts for the role of intermolecular interactions, such as π – π stacking,¹³ hydrogen bonding,¹⁴ and so on, and the influence of cocrystallized solvent molecules¹⁵ and counterions.¹⁶ Given the large number of possible variables influencing the SCO properties, it is nearly impossible to isolate their relative contributions, and weak intermolecular interactions, which also contribute to the relative stabilities of LS and HS states, can be easily overlooked.

We attempted to exclude the influence of all mentioned factors, including both size and shape variations upon SCO and relatively strong intermolecular interactions, by studying magnetic properties of compounds that do not change their

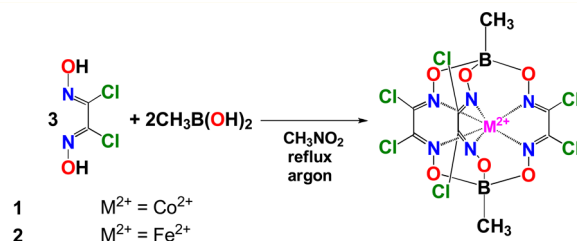


Figure 1. Synthesis of the cobalt(II) clathrochelate **1** and its diamagnetic iron(II)-containing analog **2**.

shape upon SCO; these are cobalt(II) clathrochelates (Figure 1). A macrobicyclic cage ligand determines the chemical stability of such a complex by totally encapsulating a metal ion,¹⁷ whereas the latter contributes to the complex's stability by fixing the conformation of the ligand, so the complex is not only chemically inert but also conformationally rigid.

It was recently shown that cobalt(II) hexachloroclathrochelates demonstrated the SCO¹⁸ that was gradual and incomplete in most cases. This behavior is characteristic of cobalt(II) SCO complexes,¹⁹ which rarely show significant cooperativity and volume changes upon SCO.

Surprisingly, the dissolution of the complex **1** (Figure 1), which in a solid state exhibits an incomplete and gradual SCO curve, results in a population of the purely HS state at $T > 200$ K (Figure 2), as follows from the measurements using Evans

Received: December 11, 2013

Accepted: January 17, 2014

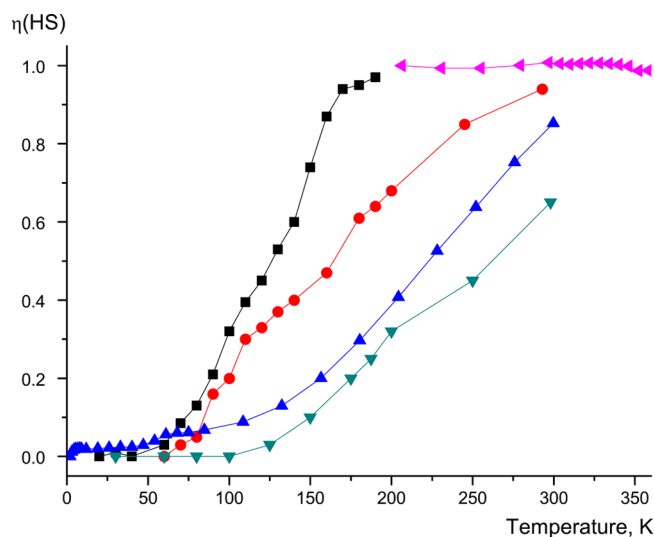


Figure 2. Temperature dependence of the HS-state population for the complex **1** in different states: single crystal (▼ (cyan), obtained by ADP analysis, Figure S6 in the SI), fine-crystalline sample (▲ (blue), obtained by measuring the magnetic susceptibility of its fine-crystalline sample, Figure S11 in the SI), extremely fine-crystalline sample (● (red), measured by integrating the EPR signal of the LS complex, Figure S3 in the SI) and its toluene solution (obtained from EPR (■, Figure S2 in the SI), and Evans method (left-facing triangle (pink), Figure S1 in the SI)).

method²⁰ (Figure S1 in the Supporting Information (SI)). Because this method, as well as direct SQUID measurement of magnetic moment of a frozen diluted solution (the latter due to a relatively low solubility), was not applicable to follow the spin crossover down to lower temperatures, we have tracked SCO down to 10 K using EPR spectroscopy by measuring the relative integral intensity of EPR signal of the LS complex (Figure S2 in the SI). According to the EPR data obtained, not only is the SCO in solution complete, it is also significantly more abrupt than that in the fine-crystalline sample. In addition, the SCO curve of the fine-crystalline sample of **1** (Figure S3 in the SI) depends on the size of crystallites;

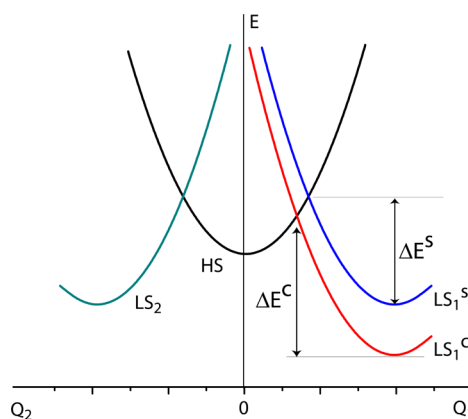


Figure 4. Sketch of an adiabatic potential energy surface along the Q_1 (stabilized by crystal packing) and Q_2 (not stabilized) coordinates. LS_1^c and LS_1^s relate to low-spin state in crystal and in solution, respectively; ΔE^c and ΔE^s correspond to the thermal spin-flip barrier in crystal and in solution, respectively.

grinding of the sample with a small amount of quartz powder shifts the SCO curve toward the one observed in solution (Figure 2).²¹ Note that the X-ray powder diffraction study did not reveal any changes in the unit cell parameters upon progressive grinding of the sample.

The multitemperature X-ray diffraction study allowed following the SCO in the single crystal of **1**. Note that the structural parameters of the caging ligand showed almost no changes upon SCO besides thermal expansion (the latter is identical for both **1** and its isostructural diamagnetic iron(II) complex **2**, Figures S4 and S5 in the SI), confirming the independence of the size and shape of **1** on the spin state. In contrast, the Co–N bond lengths of this trigonal prismatic complex reveal a significant temperature-dependent anisotropy (Figure 3), with a low-temperature distortion due to the Jahn–Teller (JT) effect in the LS complex. The increase in the temperature leads to more uniform distribution of bond lengths; however, even at RT some anisotropy remains, implying the residual population of the LS state. The rigidity of the encapsulating ligand does not favor the trans-like JT

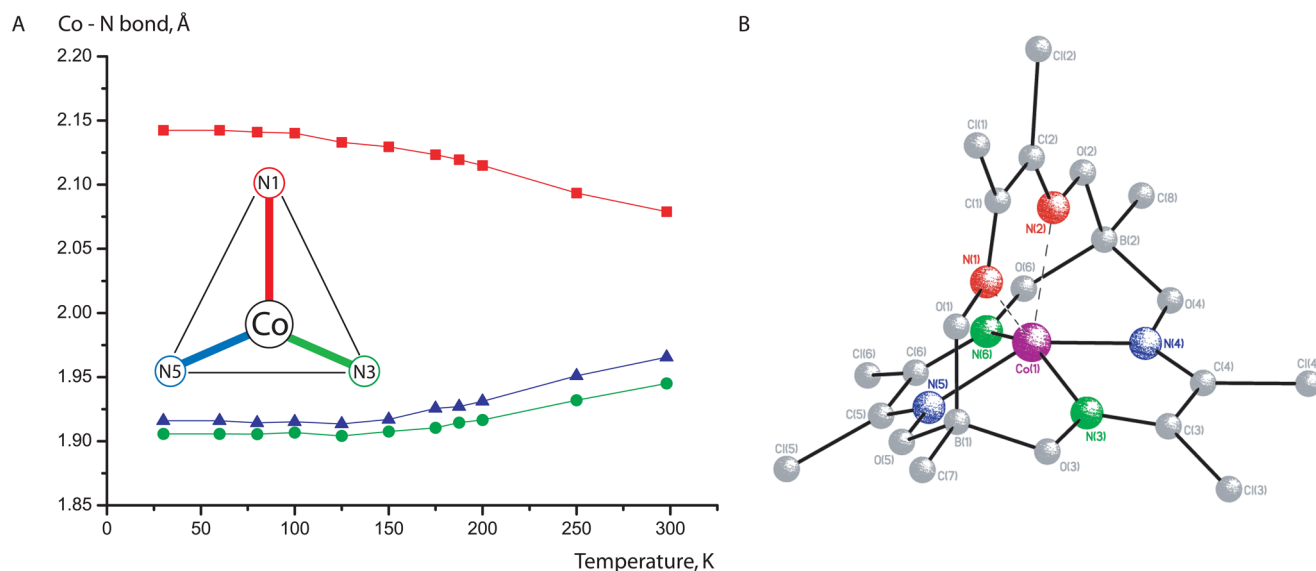


Figure 3. Temperature dependence of the Co–N bond lengths (angstroms) and a general view of the complex **1** (B) from the X-ray diffraction data.

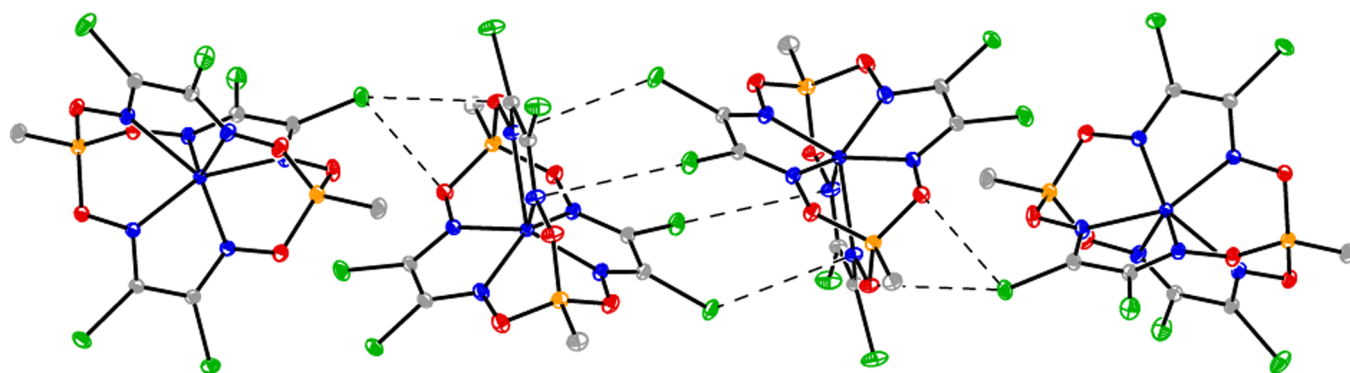


Figure 5. Fragment of the crystal packing of the compound **1** showing $\pi \cdots \text{Cl}$ intermolecular interactions in its crystal.

distortion, as it would cause excessive strain. Instead, a less common *cis*-distortion^{22,23} is observed, for which the geometry of the ligand does not change significantly, and the degeneracy is lifted by the shift of the encapsulated cobalt(II) ion from the center of the ligand's cavity toward two out of the three ribbed chelate fragments (Figure 3).

Note that atomic displacement parameters (ADPs) of the metal ion become significantly anisotropic at the temperatures higher than 100 K (in comparison with the complex **2**, Figure S6 in the SI), that is, when the HS state starts to get populated, with the most pronounced mobility observed along the direction of the JT distortion. Because this anisotropy is caused by dynamic superposition of two cobalt ion's positions corresponding to its different spin states, the analysis of ADPs allows observing the spin transition (Figure 2) in a single crystal. (See the SI for details.)

The comparison of SCO curves obtained for the sample in different states (solution, powder, and single crystal; Figure 2) suggests the stabilization of the LS state by the crystal lattice: the single crystal has the highest temperature of SCO, the progressive grinding of the sample lowers the $T_{1/2}$, and in the absence of the intermolecular interactions,²¹ that is, in a diluted solution, the $T_{1/2}$ value is the lowest and the SCO is the most abrupt. This ant cooperative^{24–26} behavior is a rather unique feature; although it was previously observed, in most cases it was explained by the difference between the conformations of a compound in solution and in crystal²⁷ or by the coordination of a solvent.²⁸ In our case, the conformational and chemical stability of clathrochelates easily rules out these hypotheses.

Indeed, purely LS clathrochelates¹⁸ display a slight twist-like distortion. In contrast, the coordination polyhedron of **1** is very close to that of a purely HS compound¹⁸ at all temperatures, suggesting that the rigid ligand framework and crystal lattice prevent the changes in the molecular shape upon SCO. In other words, the rigidity of the crystal favors the HS shape of the molecule, which rules out the possible explanation of the observed ant cooperativity by relative rigidities of the frozen solution and powder media, leading to the trapping of a compound in the LS state in the latter case.

Out of more than 30 known cobalt(II) clathrochelates (see reference in the SI), only those with six chlorine atoms in their chelate fragments can become high-spin,¹⁸ and some of them demonstrate a complete SCO without any detectable cooperativity.²⁹ Thus, the ant cooperative effects observed are due to some specific intermolecular interactions that effectively stabilize the LS state of the complex.

It is known that the LS state of a Co^{2+} ion could be strongly stabilized by vibronic $E_g \otimes e_g$ interaction;³⁰ if the crystal lattice

for some reason favors the JT distortion, the LS state should also become stabilized. For the compound studied, the Co–N bonds are nonequivalent even at the room temperature (Figure 3), so the JT distortion is static. At the same time, the temperature dependence of the EPR spectra for **1** shows that while in a fine-crystalline sample the *g*-tensor remains anisotropic up to at least 200 K (at higher temperatures the signals are broadened by relaxation, Figure S7 in the SI), the EPR signal in the frozen solution becomes isotropic already at 160 K (Figure S2 in the SI). Because the direction of the JT distortion coincides with the direction of the g_{zz} -component (as determined by the analysis of orientation-dependent EPR spectra of the diamagnetically diluted sample, Figure S8 in the SI), the loss of anisotropy can be assigned to the dynamic averaging between three equivalent JT-distorted structures.^{31,32}

Given that the JT distortion is static in crystal and is dynamic in solution, the following interpretation of the SCO behavior is suggested. The crystal lattice increases the energy barrier governing the properties of the SCO (Figure 4) by stabilizing the corresponding JT-distorted configuration. The dissolution of the complex removes intermolecular interactions, so all three JT-distorted structures have the same energy, and the LS/HS energy difference is small enough for the HS state to become populated at relatively low temperatures. While the stabilization of the LS state by a JT distortion is usually interpreted in term of binding strain concept,³³ we attempted to reveal the specific intermolecular interactions responsible for the anomaly observed. The comparison of the crystal structures of similar compounds shows that all complexes with the stabilized LS state share the same weak $\pi \cdots \text{Cl}$ interactions (Figure 5 and Figure S9 in the SI). Disrupting these interactions by either including solvent molecules into the crystal lattice¹⁸ or by using apical substituents preventing the close packing of macrobicyclic ligands²⁹ (Figure S10 in the SI) leads to the gradual and complete SCO without extra stabilization of the LS state. Although the average energy of these $\pi \cdots \text{Cl}$ interactions (estimated from X-ray diffraction data; see the SI for more details) is only 1.2 kcal/mol, the resulting weak stabilization is quite significant in comparison with the enthalpy of this LS \leftrightarrow HS transition in solution (1.7 kcal/mol using simple Boltzmann model), which explains the observed changes in the SCO curves.

Note that the energy of the stabilization of the LS state is in the range of typical values of phenomenological parameter Γ_{int}^{10} widely used in description of cooperative SCO in terms of elastic interactions, so neglecting weak intermolecular interaction leads to dramatic misjudgment of the contribution of size-dependent factors to a SCO.

By choosing a clathrochelate complex with nearly SCO-independent molecular structure in this study, we effectively eliminated the influence of elastic interactions on the SCO properties of the cobalt(II) ion, and the unique anticooperative effects of the vibronic nature have been observed for the first time. This example clearly shows how significant weak intermolecular interactions may be in determining the macroscopic magnetic properties, and ignoring them is misleading when creating prospective molecular switches. Therefore, extreme care should be taken in interpreting the SCO cooperativity in terms of elastic interactions only. The design of the SCO complexes will strongly benefit from in-depth analysis of weak intermolecular interactions, whose contribution to magnetic properties may match or even exceed that of merely size-and-shape-based factors.

■ ASSOCIATED CONTENT

● Supporting Information

Supplementary methods for NMR and EPR spectroscopy, SQUID magnetometry and X-ray crystallography. Some characteristics of intermolecular Cl $\cdots\pi$ interactions in **1**. Crystallographic data and refinement details of **1** and **2**. Temperature dependence of the effective magnetic moment of **1** in its toluene solution obtained by Evans method. Temperature dependence of the EPR spectrum of the toluene solution of **1** and fine-crystalline (grinded with a small amount of quartz powder) sample **1**. Temperature dependence of a unit cell volume for the isostructural complexes **1** and **2**. Temperature dependence of the angles between the chelate fragments of complex **1**. Temperature dependence of the largest eigenvalue of ADP matrix for the encapsulated metal ion in the isostructural complexes **1** and **2** with cobalt and iron ions, respectively. Temperature dependence of the EPR signal of the fine-crystalline sample of **1** in the Q-band. Experimental and simulated orientation-dependent EPR spectra of the diamagnetically diluted single crystal of **1** at 20 K in the X-band. Cl $\cdots\pi$ contacts in the crystal of cobalt(II) clathrochelates with *n*-buthyl and *n*-hexadecyl substituents in apical positions. Fragments of the crystal packing of the cobalt complexes with tiophenyl, pentafluorophenyl, and fluorine substituents in the capping fragments. Temperature dependence of the effective magnetic moment of the fine-crystalline powder of **1**. Additional references. This material is available free of charge via the Internet at <http://pubs.acs.org>.

■ AUTHOR INFORMATION

Corresponding Author

*E-mail: voloshin@ineos.ac.ru.

Notes

The authors declare no competing financial interest.

■ ACKNOWLEDGMENTS

This research was supported by the RFBR (grants 13-03-00732, 13-03-92691, 13-03-12197, 14-03-00224, and 14-03-31604), CPRF (grants MK-4842.2013.3, MD-276.2014.3), and RAS (program 6). We thank A. S. Belov, A. O. Dmitrienko, N. V. Efimov, and G. V. Romanenko for the technical assistance.

■ REFERENCES

- (1) Sato, O.; Tao, J.; Zhang, Y. Z. Control of Magnetic Properties Through External Stimuli. *Angew. Chem., Int. Ed.* **2007**, *46*, 2152–2187.
- (2) Gütllich, P.; Garcia, Y.; Goodwin, H. A. Spin Crossover Phenomena in Fe(II) Complexes. *Chem. Soc. Rev.* **2000**, *29*, 419–427.
- (3) Miyamachi, T.; Gruber, M.; Davesne, V.; Bowen, M.; Boukari, S.; Joly, L.; Scheurer, F.; Rogez, G.; Yamada, T. K.; Ohresser, P.; Beaurepaire, E. et al. Robust Spin Crossover and Memory Across a Single Molecule. *Nat. Commun.* **2012**, *3*.
- (4) Halder, G. J.; Kepert, C. J.; Moubaraki, B.; Murray, K. S.; Cashion, J. D. Guest-Dependent Spin Crossover in a Nanoporous Molecular Framework Material. *Science* **2002**, *298*, 1762–1765.
- (5) Cavallini, M.; Bergenti, I.; Milita, S.; Ruani, G.; Salitros, I.; Qu, Z. R.; Chandrasekar, R.; Ruben, M. Micro- and Nanopatterning of Spin-Transition Compounds into Logical Structures. *Angew. Chem., Int. Ed.* **2008**, *47*, 8596–8600.
- (6) Gütllich, P.; Goodwin, H. A. *Spin Crossover in Transition Metal Compounds I–III*; Springer: New York, 2004; Vols. 233–235.
- (7) Kahn, O.; Martinez, C. J. Spin-transition Polymers: From Molecular Materials Toward Memory Devices. *Science* **1998**, *279*, 44–48.
- (8) Bao, X.; Leng, J. D.; Meng, Z. S.; Lin, Z.; Tong, M. L.; Nihei, M.; Oshio, H. Tuning the Spin States of Two Apical Iron(II) Ions in the Trigonal-bipyramidal [Fe(II)(μ-bpt)₃]2Fe(II)(μ₃-O)]²⁺ Cations through the Choice of Anions. *Chem.—Eur. J.* **2010**, *16*, 6169–74.
- (9) Gütllich, P.; Hauser, A.; Spiering, H. Thermal and Optical Switching of Iron(II) Complexes. *Angew. Chem., Int. Ed. Engl.* **1994**, *33*, 2024–2054.
- (10) Spiering, H.; Meissner, E.; Koppen, H.; Müller, E. W.; Gütllich, P. The Effect of the Lattice Expansion on High-Spin Reversible Low-Spin Transitions. *Chem. Phys.* **1982**, *68*, 65–71.
- (11) Sinitskiy, A. V.; Tchougreff, A. L.; Dronskowski, R. Phenomenological Model of Spin Crossover in Molecular Crystals as Derived from Atom-Atom Potentials. *Phys. Chem. Chem. Phys.* **2011**, *13*, 13238–13246.
- (12) Halcrow, M. A. Structure:Function Relationships in Molecular Spin-Crossover Complexes. *Chem. Soc. Rev.* **2011**, *40*, 4119–4142.
- (13) Real, J. A.; Gaspar, A. B.; Niel, V.; Munoz, M. C. Communication Between Iron(II) Building Blocks in Cooperative Spin Transition Phenomena. *Coord. Chem. Rev.* **2003**, *236*, 121–141.
- (14) Weber, B.; Bauer, W.; Pfaffeneder, T.; Dirtu, M. M.; Naik, A. D.; Rotaru, A.; Garcia, Y. Influence of Hydrogen Bonding on the Hysteresis Width in Iron(II) Spin-Crossover Complexes. *Eur. J. Inorg. Chem.* **2011**, 3193–3206.
- (15) Reger, D. L.; Gardinier, J. R.; Smith, M. D.; Shahin, A. M.; Long, G. J.; Rebbouh, L.; Grandjean, F. Polymorphism in Fe[(p-IC₆H₄)B(3-Mepz)(3)](2) (pz = pyrazolyl): Impact of Supramolecular Structure on an Iron(II) Electronic Spin-State Crossover. *Inorg. Chem.* **2005**, *44*, 1852–1866.
- (16) Yamada, M.; Ooidemizu, M.; Ikuta, Y.; Osa, S.; Matsumoto, N.; Iijima, S.; Kojima, M.; Dahan, F.; Tchuagues, J. P. Interlayer Interaction of Two-Dimensional Layered Spin Crossover Complexes [(FeH₃)-H-II L-Me] [(FeLMe)-L-II]X (X = ClO₄, BF₄, PF₆, AsF₆, and SbF₆; H₃LMe = tris[2-(((2-methylimidazol-4-yl)-methylidene)amino)ethyl]amine. *Inorg. Chem.* **2003**, *42*, 8406–8416.
- (17) Voloshin, Y. Z.; Varzatskii, O. A.; Vorontsov, I. I.; Antipin, M. Y. Tuning a Metal's Oxidation State: The Potential of Clathrochelate Systems. *Angew. Chem., Int. Ed.* **2005**, *44*, 3400–3402.
- (18) Voloshin, Y. Z.; Varzatskii, O. A.; Novikov, V. V.; Strizhakova, N. G.; Vorontsov, I. I.; Vologzhanina, A. V.; Lyssenko, K. A.; Romanenko, G. V.; Fedin, M. V.; Ovcharenko, V. I.; et al. Tris-Dioximate Cobalt(I,II,III) Clathrochelates: Stabilization of Different Oxidation and Spin States of an Encapsulated Metal Ion by Ribbed Functionalization. *Eur. J. Inorg. Chem.* **2010**, 5401–5415.
- (19) Krivokapic, I.; Zerara, M.; Daku, M. L.; Vargas, A.; Enachescu, C.; Ambrus, C.; Tregenna-Piggott, P.; Amstutz, N.; Krausz, E.; Hauser, A. Spin-Crossover in Cobalt(II) Imine Complexes. *Coord. Chem. Rev.* **2007**, *251*, 364–378.
- (20) Evans, D. F. The Determination of the Paramagnetic Susceptibility of Substances in Solution by Nuclear Magnetic Resonance. *J. Chem. Soc.* **1959**, 2003–2005.

- (21) Haddad, M. S.; Federer, W. D.; Lynch, M. W.; Hendrickson, D. N. Spin-Crossover Ferric Complexes: Unusual Effects of Grinding and Doping Solids. *J. Am. Chem. Soc.* **1981**, 131–139.
- (22) Echeverría, J.; Cremades, E.; Amoroso, A. J.; Alvarez, S. Jahn-Teller Distortions of Six-Coordinate CuII Compounds: Cis or Trans? *Chem. Commun.* **2009**, 4242–4.
- (23) Cremades, E.; Echeverría, J.; Alvarez, S. The Trigonal Prism in Coordination Chemistry. *Chem.—Eur. J.* **2010**, 16, 10380–10396.
- (24) Scott, H. S.; Ross, T. M.; Chilton, N. F.; Gass, I. A.; Moubaraki, B.; Chastanet, G.; Paradis, N.; Letard, J. F.; Vignesh, K. R.; Rajaraman, G.; Battena, S. R.; Murray, K. S. Crown-Linked Dipyritylamino-Triazine Ligands and Their Spin-Crossover Iron(II) Derivatives: Magnetism, Photomagnetism and Cooperativity. *Dalton Trans.* **2013**, 42, 16494–16509.
- (25) Real, J. A.; Bolvin, H.; Bousseksou, A.; Dworkin, A.; Kahn, O.; Varret, F.; Zarembowitch, J. 2-Step Spin Crossover in the New Dinuclear Compound [Fe(Bt)(Ncs)2]2bpym, with Bt = 2,21'-Bi-2-Thiazoline and Bpym = 2,2'-Bipyrimidine - Experimental Investigation and Theoretical Approach. *J. Am. Chem. Soc.* **1992**, 114, 4650–4658.
- (26) Bolvin, H.; Kahn, O. Cooperativity and Anticooperativity in Spin Transition Compounds - Macroscopic Approach and Orbital Modelization. *Mol. Cryst. Liq. Cryst. Sci. Technol., Sect. A* **1993**, 234, 275–282.
- (27) Jenkins, D. M.; Peters, J. C. Spin-State Tuning at Pseudotetrahedral d(7) Ions: Examining the Structural and Magnetic Phenomena of Four-Coordinate [BP3]CoII-X Systems. *J. Am. Chem. Soc.* **2005**, 127, 7148–65.
- (28) Toftlund, H. Spin Equilibrium in Solutions. *Monatsh. Chem.* **2001**, 132, 1269–1277.
- (29) Belov, A. S.; Dolganov, A. V.; Novikov, V. V.; Vologzhanina, A. V.; Fedin, M. V.; Kuznetsov, E. V.; Bubnov, Y. N.; Voloshin, Y. Z. Template Synthesis, Structure and Electropolymerization of the 2-Thiopheneboron-Capped Cobalt(II) Clathrochelates. *Inorg. Chem. Commun.* **2013**, 29, 160–164.
- (30) Reinen, D.; Atanasov, M. The Influence of Jahn–Teller Coupling on the High-Spin/Low-Spin Equilibria of Octahedral MIIIL6 Polyhedra (MII: Mn – Cu), with NiF6 3– as the Model Example. In *The Jahn-Teller Effect*; Köppel, H., Yarkony, D. R., Barentzen, H., Eds.; Springer: Berlin Heidelberg, 2009; Vol. 97, pp 451–486.
- (31) Kundu, T. K.; Manoharan, P. T. An Electron Paramagnetic Resonance Investigation of a Macrobicyclic Cage Complex of Ag(II). Dynamic and Static Jahn-Teller Distortions. *Chem. Phys. Lett.* **1997**, 264, 338–344.
- (32) Nielsen, P.; Toftlund, H.; Bond, A. D.; Boas, J. F.; Pilbrow, J. R.; Hanson, G. R.; Noble, C.; Riley, M. J.; Neville, S. M.; Moubaraki, B.; Murray, K. S. Systematic Study of Spin Crossover and Structure in [Co(terpyRX)(2)](Y)(2) Systems (terpyRX=4'-alkoxy-2,2':6',2''-terpyridine, X=4, 8, 12, Y = BF4-, ClO4-, PF6-, BPh4-). *Inorg. Chem.* **2009**, 48, 7033–7047.
- (33) Reinen, D.; Atanasov, M.; Kohler, P.; Babel, D. Jahn-Teller Coupling and the Influence of Strain in T-g and E-g Ground and Excited States - a Ligand Field and DFT Study on Halide (MX6)-X-III Model Complexes [M = Ti-III-Cu-III, X = F-, Cl-]. *Coord. Chem. Rev.* **2010**, 254, 2703–2754.